Amorphous and nanophase microstructures of bulk Se-based chalcogenide alloys

Abhay Kumar Singh*

Department of Physics, Indian Institute of Science, Bangalore 560012, India

(Received 14 January 2012)

The composition-dependent microstructural morphology variations of $Se_{89}Zn_2Te_5In_4$ and $Se_{87}Zn_2Te_5In_6$ chalcogenide alloys are investigated. Glassy and nanophase surfaces and structural morphologies of these alloys have been described with help of scanning electron microscope (SEM) and transmission electron microscope (TEM), and their elemental concentrations are confirmed from the energy dispersive X-ray spectroscopy (EDX). Experimental results demonstrate that the microstructure of $Se_{89}Zn_2Te_5In_4$ alloy belongs to pure glassy state, while the $Se_{87}Zn_2Te_5In_6$ alloy is with nanophase structure.

Document code: A **Article ID:** 1673-1905(2012)03-0165-3

DOI 10.1007/s11801-012-2010-6

Nano-embedded chalcogenide glasses (ChG) or amorphous semiconductors have been the extensive research topic recently[1,2] due to their potential applications in high speed nano-electronics. ChG are multifunctional, so they can be used for threshold switches[3], memory elements, optical fibers[4-6], functional elements in integrated-optic circuits[7], nonlinear optics[8], holographic and memory storage media[9,10], chemical and bio-sensors[11,12] and infrared photovoltaics[13], etc.

Study of nanophase separation in multicomponent ChG is getting much attention in material science[1,5], to deduce the potential materials like nano-crystalline and nano-embedded ChG. The nanophase not only induces pronounced effects on physical properties of materials, but also influences their working performance. Therefore, it is useful to have a good understanding on the nanophase formation within the microstructure in ChG and its effect on physical properties of the materials.

Non-metal, metal and semi-metal containing multicomponent chalcogenide alloys have become attractive compositions owing to their enhanced thermal, electrical and optical properties. In order to achieve such composition multicomponent alloys, we also demonstrated Se-Zn-Te-In alloys and performed study on their physical variations[14-16]. Specifically, the significant changes in thermal stability[14], electrical conductivity[15] and UV/visible & IR-transmission [16] are getting much attention. The results of previous studies on Se-Zn-Te-In multicomponent ChG[14-16] demonstrated that the thermal, electrical and optical parameters have been drastically changed at 6 atomic percentage of indium. The drastic change in physical properties of $Se_{87}Zn_2Te_5In_6$ composition alloy has arisen due to nanophase formation within the glassy microstructure.

In this paper, the composition-dependent scanning electron microscopic (SEM) and transmission electron microscopic (TEM) microstructural analyses of $Se_{89}Zn_2Te_5In_4$ and $Se_{87}Zn_2Te_5In_6$ ChG are reported. Subsequently, alloying elemental concentrations have been confirmed from the energy dispersive X-ray spectroscopy (EDX) analysis.

Bulk amorphous and nanophase glassy materials were prepared by conventional melting quenched technique. High-purity (99.999%) elements of selenium, zinc, tellurium and indium were used, which purchased from alfa aesar. The desired amount of elements was weighed by electronic balance and put into cleaned quartz ampoules with the length of 8 cm and the diameter of 14 mm. The ampoules were evacuated and sealed under a vacuum of 10^{-5} Torr to avoid the reaction of glasses with oxygen at high temperature. A bunch of sealed ampoules was continuously heated in electric furnace with 1173 K at the rate of 5−6 K/min and held at that temperature for 10−11 h. During the melting process, the ampoules were frequently rocked with interval of 30 min to ensure the diffusion homogeneity of molten materials. After achieving the desired melting time, the ampoules with molten materials were frequently quenched into ice-cooled water[16].

Microstructural characterizations were performed by us-

* E-mail: abhaysngh@rediffmail.com

ing SEM with high resolution (JEOL 840A model with KEVEX-EDX attachment) in magnification range of 1000×. To prevent the conducting nature of specimens, gold coating was used. However, TEM images of prepared samples were obtained from the FEI, TECNAI 20G^2. For the TEM analysis, the powder sample floated in fresh water which is invisible from naked eyes, and it was picked from the copper grids.

In Fig.1(a), SEM microstructure of $Se_{89}Zn_2Te_5In_4$ glass is shown, and it is fractured, rough and dry, while the SEM microstructure of $Se_{87}Zn_2Te_5In_6$ glass exhibits comparatively lush and fractured surface morphology as shown in Fig.1(b). Such a compact and lush SEM microstructure of $Se_{87}Zn_2Te_5In_6$ arises due to the higher steric hindrance in alloy configuration. The SEM microstructural studies reveal that the $Se_{89}Zn_2Te_5In_4$ alloy has comparatively inferior physical properties than the $Se_{87}Zn_2Te_5In_6$ alloy. This interpretation of SEM microstructural observation is also consistent with past studies about the electrical, thermal stability and optical parameters of Se-Zn-Te-In ChG[14-16].

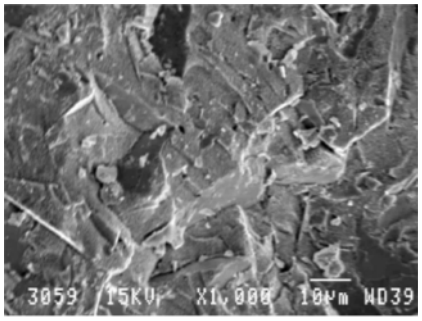

(a) $Se_{89}Zn_2Te_5In_4$

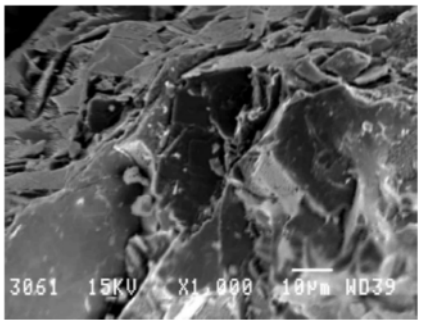

(b) $Se_{87}Zn_2Te_5In_6$

Fig.1 SEM microstructures of $Se_{89}Zn_2Te_5In_4$ and $Se_{87}Zn_2Te_5In_6$ bulk chalcogenide alloys at resolution of 1000×

TEM microstructure and selected area electron diffraction (SAED) pattern of $Se_{89}Zn_2Te_5In_4$ composition glass are given in Fig.2. TEM microstructure of this composition alloy shows homogeneous morphology, and the corresponding SAED (inset of Fig.2) image exhibits a clear ring structure without any bright spot. This composition alloy only has glassy structures, and there is no clear evidence for nanophase formation within the microscopic morphology. However, TEM microstructure of $Se_{87}Zn_2Te_5In_6$ system shown in Fig.3 exhibits very fine crystallization growth within the glassy morphology. SAED image (inset of Fig.3) of this composition alloy also verifies the observation by showing the fine bright spots between two conjunctive rings. Thus TEM and SAED analyses reveal the clear evidences for nanophase formation within the microscopic structure of $Se_{87}Zn_2Te_5In_6$ composition glass.

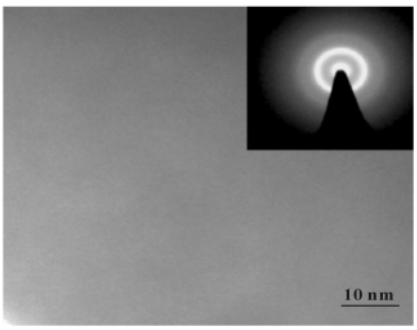

Fig.2 TEM image and SAED pattern of amorphous $Se_{89}Zn_2Te_5In_4$ chalcogenide glass

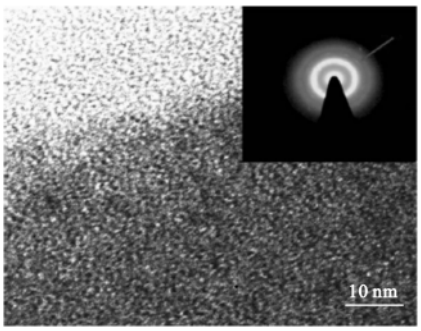

Fig.3 TEM image and SAED pattern of nano-embedded $Se_{87}Zn_2Te_5In_6$ chalcogenide glass

To ensure the elemental concentration of glassy and nanophase glassy alloys, the energy dispersive X-spectroscopy (EDX) measurements were also performed. EDX patterns of studied alloys are given in Fig.4. The EDX pattern of $Se_{89}Zn_2Te_5In_4$ glassy alloy shows the SeL_α & SeL_β phases with high elemental concentration and InL_α & InL_β and TeL_α & TeL_β phases with lower compositional amounts. The EDX pattern of nano-embedded $Se_{87}Zn_2Te_5In_6$ glassy alloy also shows the Se L_α & SeL_β intense and other InL_α, InL_β, TeL_α and TeL_β with low concentrations. High counts of SeL_α, SeL_β, and InL_α, InL_β elemental phases for optimum composition arise due to the large number of unsaturated bonds under the influence of reducing and increasing compositional amounts of Se and In. It might be accounted to produce the microstructural variation within the glassy morphology. Here the peak of element Zn does not

appear in both EDX patterns of systems, owing to alloying element concentration is below the detection limit of instrument.

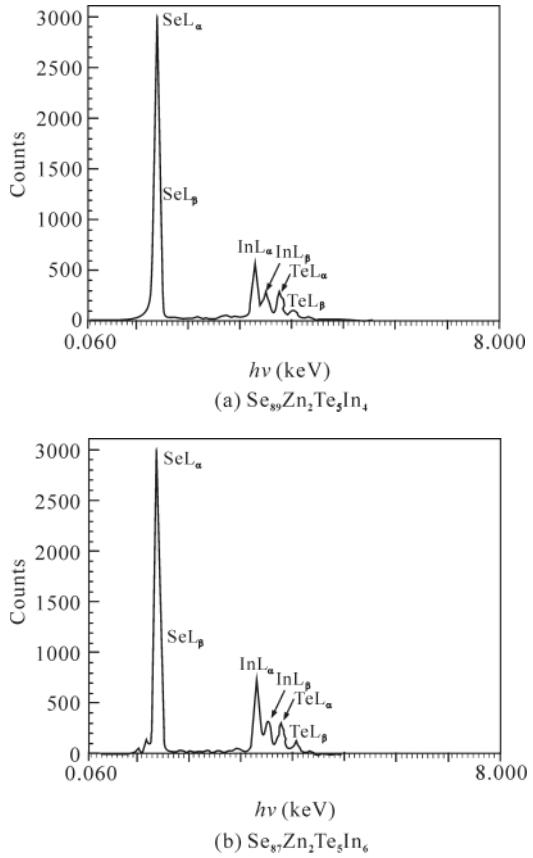

Fig.4 EDX patterns of $Se_{89}Zn_2Te_5In_4$ glassy chalcogenide alloy and $Se_{87}Zn_2Te_5In_6$ nanophase glassy chalcogenide alloy

The composition-dependent microstructure variations in SEM, TEM, SAED and EDX of $Se_{89}Zn_2Te_5In_4$ and $Se_{87}Zn_2Te_5In_6$ alloys can be demonstrated with help of bond theory of solids. It is expected that the metallic Zn, metallic chalcogen element Te and semi-metallic In bonds dissolve in Se chains, which possibly makes Zn-Zn, Te-Te, Se-Se, In-In, Se-Zn, Se-Te, Zn-Te, Se-In, Se-Zn-Te-In homopolar and heteropolar bonds with cross-linked metastable state structure. The Se-In heteropolar bonds play an important role in morphology variation owing to the fixed amounts of Zn and Te[17]. Incorporation of additional amount of indium increases the steric hindrance in glassy configuration and produces large number of defects in density of localized states[18,19]. As a result, high order cross-linking has occurred in the configuration of $Se_{87}Zn_2Te_5In_6$ alloy. The existance of large number of defects or vacancies[20, 21] influences the microstructure of glassy alloy and accounts for nanophase formation within the morphology of $Se_{87}Zn_2Te_5In_6$ alloy.

In conclusion, the composition-dependent microstructural transformations of $Se_{89}Zn_2Te_5In_4$ and $Se_{87}Zn_2Te_5In_6$ ChG alloys are discussed. TEM and SAED experimental observations reveal that the $Se_{89}Zn_2Te_5In_4$ composition alloy is a pure glassy material, while $Se_{87}Zn_2Te_5In_6$ composition alloy can grow the nanophase (or nano-embedded) structure within the homogeneous glassy morphology. It is also obtained that the EDX pattern elemental phase counts and the intensity of nanophase alloy are higher than those of pure amorphous alloy, owing to the existence of larger number of unsaturated heteropolar hydrogen-like bonds in localized states.

References

[1] K. Tanaka, J. Non-Cryst. Solids **326&327**, 21 (2003).
[2] S. Juodkazis, H. Misawa, O. A. Louchev and K. Kitamura, Nanotechnology **17**, 4802 (2006).
[3] V. C. Selvaraju, S. Asokan and V. Srinivasan, Appl. Phys. A **77**, 149 (2003).
[4] K. Shportko, S. Kremers, M. Woda, D. Lencer, J. Robertson and M. Wuttig, Nature Materials **7**, 653 (2008).
[5] D. J. Milliron, S. Raoux, R. M. Shelby and J. J. Sweet, Nature Materials **6**, 352 (2007).
[6] B. F. Bowden and J. A. Harrington, Applied Optics **48**, 3050 (2009).
[7] M. Pelusi, F. Luan, T. D. Vo, M. R. E. Lamont, S. J. Madden, D. A. Bulla, D. Y. Choi, B. L. Davies and B. J. Eggleton, Nature Photonics **3**, 139 (2009).
[8] J. M. Dudley and J. R. Taylor, Nature Photonics **3**, 85 (2009).
[9] V. Vassilev, K. Tomova, V. Parvanova and S. Boycheva, J. Alloys and Comp. **485**, 569 (2009).
[10] M. Wuttig and N. Yamada, Nature Materials **6**, 824 (2007).
[11] J. Schubert, M. J. Schoning, Y. G. Mourzina, A. V. Legin, Y. G. Vlasov, W. Zander and H. Luth, Sensor and Actuators **76**, 327 (2001).
[12] M. L. Anne, J. Keirsse, V. Nazabal, K. Hyodo, S. Inoue, C. B. Pledel, H. Lhermite, J. Charrier, K. Yanakata, O. Loreal, J. L. Person, F. Colas, C. Compere and B. Bureau, Sensors **9**, 7398 (2009).
[13] E. H. Sargent, Nature Photonics **3**, 325 (2009).
[14] A. K. Singh, N. Mehta and K. Singh, Philo. Mag. Lett. **90**, 201 (2010).
[15] A. K. Singh, N. Mehta and K. Singh, Chalcogenide Lett. **6**, 9 (2009).
[16] A. K. Singh, N. Mehta and K. Singh, Physica B **404**, 3470 (2009).
[17] A. K. Singh and K. Singh, Eur. Phys. J. Appl. Phys. **51**, 30301 (2010).
[18] R. M. Abdel Latif, Physica B **254**, 273 (1998).
[19] G. Saffarini, Appl. Phys. A **74**, 283 (2002).
[20] M. Wuttig, D. Lüsebrink, D. Wamwangi, W. We.nic, M. Gilleben and R. Dronskowski, Nature Materials **6**, 122 (2007).
[21] A.V. Kolobov and J. Tominaga, J. Opto. and Adv. Mater. **4**, 679 (2002).